ARTICLE

Mucin Coated Protein-Polyphenol Microcarriers for Daidzein Delivery

pReceived 00th January 20xx,
Accepted 00th January 20xx

DOI: 10.1039/x0xx00000x

Su Hui Lim*[a], Germaine Jia Min Yong[a,b], Cheryl Yingxue Chia [a], Shu Mei Man [a], Gomathy Sandhya Subramanian [a], Geraldine Oh [a], Eleanor Jing Yi Cheong [a] and Maxim V. Kiryukhin*[a,c]

Daidzein, an isoflavone found abundantly in legumes, may benefit from bypassing upper gut absorption to reach the colon where it can be metabolized into the potent estrogen equol by the gut microbiome. To achieve this, we developed mucin coated protein-tannin multilayer microcarriers. Preliminary screening of several types of mucin coatings was performed by following the *in vitro* digestion of microcarriers encapsulating DQ-Red bovine serum albumin (BSA) using fluorescence spectroscopy. Mucin type III from porcine stomach was found to provide the highest protection against intestinal digestion. Raman spectroscopy confirmed mucin-tannin complexation involving both hydrophobic interactions and hydrogen bonding. Highly porous functionalized calcium carbonate (FCC) microparticles efficiently absorbed daidzein from a dimethyl sulfoxide (DMSO) solution, with a loading capacity of 21.6 ± 1.8 wt.% as measured by ultra-high pressure liquid chromatography – mass spectrometry (UPLC-MS). Daidzein-containing FCC microparticles were then coated with BSA-tannin n-layer film and mucin ($(BSA\text{-}TA)_n$-mucin) by Layer-by-Layer deposition from corresponding aqueous solutions followed by FCC decomposition with HCl. The resulting multilayer microcarriers contained 54 wt.% daidzein as confirmed by X-ray diffraction and UPLC-MS. *In vitro* digestion testing using the INFOGEST model showed that $(BSA\text{-}TA)_8$-mucin and $(BSA\text{-}TA)_4$-mucin microcarriers retained 71 ± 8.2 % and 68 ± 2.3 % of daidzein, respectively, at the end of the small intestinal phase. Mucin-free $(BSA\text{-}TA)_8$ retained lower daidzein amount of 46 ± 4.6 %. Therefore, mucin coating improved daidzein retention in protein-tannin microcarriers by 54 % during digestion. Release daidzein and conversion into equol were observed during *in-vitro* colonic studies with donor fecal microbiota from a healthy non-equol-producing donor and *Slackia equolifaciens*. This approach has the potential for encapsulating other hydrophobic nutraceuticals or therapeutics, enhancing their bioaccessibility in the colon.

1. Introduction

Daidzein, a type of isoflavone found abundantly in legumes, particularly soy[1, 2], has been associated with various potential health benefits including antioxidant[3, 4], anti-inflammatory[5, 6] and anti-cancer[7, 8] properties. It is a small hydrophobic molecule soluble in polar solvents but with very low aqueous and lipid solubility. Therefore, the oral bioavailability[9-11] and bioaccessibility[12-14] for further metabolism are both poor which limits its beneficial impact. Recently, there were a number of studies published on daidzein delivery systems aiming to enhance its passive diffusion through intestinal epithelium by exploiting nanocarriers, e.g., solid lipid nanoparticles[15], cyclodextrin complexes[16], polylactic acid nanoparticles [17], liposomes[18] and solid dispersions.[19] However, it may be beneficial to deliver daidzein intact to the colon bypassing its absorption in the upper gastrointestinal tract. A significant percentage of people, ranging from 20 to 60 % across geographical populations, have gut microbiomes that convert daidzein into equol[20, 21], which has exponentially greater antioxidant[22] and enzyme-inhibitory properties[23] than its precursor. Equol has been shown to alleviate osteoporosis, menopausal symptoms, and lower prostate cancer risk.[24]

Many of the existing carriers aiming colon delivery are designed to achieve pH-, time- or pressure-based releases mechanisms.[25, 26] The main disadvantage of these release triggers is their limited specificity where release of encapsulated compound can be unpredictable. Recently, Sanatkar *et. al.*[7] reported an approach to deliver daidzein to the colon using chitosan capsules susceptive to degradation by enzymes of colonic bacteria. They reported chitosan microcapsules with 64.3 % entrapment efficiency and cumulative release of 38 % in simulated gastric fluid (SGF, pH 4.5), 58 % after subsequent treatment in simulated intestinal fluid (SIF, pH 6.8) and 79 % in simulated colonic fluid (pH 6.8 – 7).

Our group is developing microencapsulation systems where release is triggered by components specific to various sections of the gastrointestinal tract.[27-30] We have reported layer-by-layer (LbL) assembled protein-polyphenol microcarriers for protection against gastric digestion of a bioactive ingredient, lactoferrin, and its controlled release in the small intestine triggered by proteolysis of the protein component of the shells

[a] Singapore Institute of Food and Biotechnology Innovation (SIFBI), Agency for Science, Technology and Research (A*STAR), 31 Biopolis Way, #01-02 Nanos, Singapore 138669. Email: maximkir@msn.com; Lim_Su_Hui@sifbi.a-star.edu.sg
[b] Asian Microbiome Library Pte. Ltd., 89 Science Park Dr, #03-09, Singapore 118261.
[c] Life Improvement by Future Technologies (LIFT) Center, 143025, Moscow, Russia

with an intestinal protease, α-chymotrypsin.[27, 29] Furthermore, we have also reported the incorporation of a whey protein, immunoglobulin G, into the LbL assembled microcarriers which dramatically increased their adhesion towards intestinal epithelial to achieve sustained release.[28] Functionalized calcium carbonate (FCC) was suggested as a template material offering several benefits, including it is food grade, cost-efficient (compared with porous silica or others) and has extremely high porosity.[31, 32] This means that FCC is capable of efficiently accommodating a significant amount of active ingredients within its structure in food application when compared to vaterites and other types of calcium carbonate.

Recently, Butnarasu *et. al.*[33] has reported mucosomes (a novel class of glycosylated nanoparticles based on mucin) as a multi-drug delivery platform for pharmacological treatments. The mucosomes appeared to be resistant to proteolytic activity of intestinal proteases delaying release of encapsulated ingredient for 2 hours, which is typical duration of the intestinal digestion phase.[34]

In this paper, we will test an idea to modify protein-polyphenol microcarriers with a terminal layer of mucin aiming to enhance their stability in the small intestine. We will study the type of mucin best-suited for this purpose and the mucin-polyphenol binding mechanisms. We will describe a newly developed method of daidzein loading into the FCC that overcomes challenges associated with low daidzein solubility in both water and lipids. We will analyse the loading capacity of FCC for daidzein and its retention efficiency during established in-vitro INFOGEST model simulating digestion conditions along the gastrointestinal tract. We hypothesise that this design of microcarriers will enhance bioacessibility of daidzein to the colonic microbiome to maximize its conversion to equol.

2. Materials and Methods

2.1 Materials

Functionalized Calcium Carbonate (FCC) was provided by Omya International AG, Switzerland. Daidzein powder was purchased from MedChemExpress (Princeton, NJ). Bovine Serum Albumin (BSA) lyophilized powder (≥96 %), tannic acid (TA) ACS grade, mucin type I-S from bovine submaxillary glands, mucin type II from porcine stomach, mucin type III from porcine stomach (bound sialic acid 0.5-1.5 % partially purified powder), hydrochloric acid ACS 37 %, and dimethyl sulfoxide (DMSO) ACS Reagent ≥99.9 % were purchased from Sigma-Aldrich. DQ™ Red BSA was purchased from Molecular Probes Inc, USA. Alpha-amylase from human saliva (type XI), bile salts (for microbiology), pancreatin from porcine pancreas (≥100 USP U/mg), pepsin from porcine gastric mucosa (lyophilized powder, 3200–4500 units/mg protein), calcium chloride dihydrate (≥99.0 %), magnesium chloride hexahydrate (ACS reagent, 99.0 - 102.0 %), monopotassium phosphate (≥99.0 %), potassium chloride (anhydrous, free flowing, ReagentPlus®, ≥99 %), mini protease inhibitor cocktail cOmplete™, ammonium carbonate (ACS reagent, ≥30 % NH3 basis), sodium chloride (anhydrous, free flowing, ACS reagent, ≥99 %), sodium hydroxide (Reagent grade, ≥98 % pellets anhydrous), sodium bicarbonate (for microbiology), formic acid were purchased from Sigma-Aldrich. Daidzein-d3 was purchased from Cambridge Isotopes Laboratories (Andover, MA). Analytical grade acetonitrile and methanol were purchased from Thermofisher Scientific. All chemicals were used as received without further purification. Deionized (DI) water (specific resistivity higher than 18.2 MΩcm) from Milli-Q plus 185 (Millipore) water purification system was used to make all the aqueous solutions.

2.2 Layer-by-Layer (LbL) assembly of mucin-terminated microcarriers

Loading 300 mg of porous FCC microparticles in 3 mL of 50 mg/mL daidzein solution in DMSO or 1.5 mL of 1 mg/mL DQ-red-BSA aqueous solution and shaken for 15 minutes. Next, the supernatant and microparticles were separated by centrifugation at 3000 rpm for 3 minutes and washed once or twice with 5 mL of DMSO solution or DI water, respectively. The wet cake was dried in vacuum oven for 4 hours at 60 °C. LbL assembly of BSA-TA shells begins with either 30 mg daidzein loaded FCC powder or 60 mg of DQ-red BSA loaded FCC powder suspended in 5 mL of BSA (2 mg/ml) and shaken for 15 minutes. The supernatant and microcarriers were separated by centrifugation at 3000 rpm for 5 minutes followed by two washing steps with DI water. Next, 5 mL of 3 mg/ml TA solution was introduced to the microcarriers and shaken for 15 minutes following centrifugation with two DI water washing steps. This procedure was repeated to achieve 4 or 8 BSA-TA bilayers. For the terminal layer, 5 ml solution of 2 mg/ml of either mucin I, II or III was introduced and shaken for 15 minutes, following centrifugation at 3000 rpm for 5 minutes followed by two DI water washing steps. After completion of LbL assembly, the microcarriers were re-dispersed in 5 mL of DI water. 1M HCl was slowly added under agitation until pH of suspension reaches 2.5. This was done to decompose the core FCC. Subsequently, the microcarriers were washed with DI water till pH ~6.0, separated from the supernatant by centrifugation, and the obtained wet cake was freeze-dried.

2.3 INFOGEST of mucin-terminated microcarriers

Simplified INFOGEST method[35] was used for in-vitro upper gut digestion of DQ-red-BSA loaded microcarriers for preliminary screening of different type of mucin-terminated microcarriers. All experiments were done at 37 °C under continuous agitation. Simulated gastric fluid (SGF) was prepared by adding of 1 mL of 7.1 mg/mL pepsin solution to 4 mL of 150 mM NaCl solution (acidified to pH 3). The freeze-dried microcarriers were suspended in 5 mL of DI water and added into SGF to start gastric digestion for 120 minutes. Samples were collected at every 60 minutes and digestion was stopped by adding protease inhibitor solution. After 120 minutes of gastric digestion, pH was increased to 7 by addition of 0.1M $NaHCO_3$ solution. Next, 1 mL of pancreatin (18 mg/mL in 0.1M $NaHCO_3$ solution at pH 7, pancreatin final concentration was 12 USP U/mg) solution and 1 mL of bile salt (120 mM in of 0.1M $NaHCO_3$ solution at pH 7) solution were added as simulated intestinal fluid (SIF), which mark the start of 120 minutes intestinal digestion. Samples

were collected at every 30 minutes and digestion was stopped by adding protease inhibitor solution.

Full INFOGEST method[34] was used for in-vitro upper gut digestion of daidzein loaded microcarriers. All experiments were conducted in individual tube setup of simulated salivary fluid (SSF), SGF and SIF phases. Digestion of each prototype was done in triplicate using 5 mg of microcarriers. SSF solution at pH 7 was prepared by adding 1.89 mL of 0.5M KCl solution, 462.50 µL of 0.5M KH_2PO_4 solution, 850 µL of 1M $NaHCO_3$ solution, 7.50 µL of 0.15M $MgCl_2$ solution, 7.5 µL of 0.5M $(NH_4)_2CO_3$ solution, 11.25 µL of 1M HCl solution, 3.125 µL of 0.3M $CaCl_2$ solution and 46.72 mL of DI water. In the salivary digestion setup, 1 mL of 5 mg/mL of microcarriers with oral master mix consisting of 0.748 mL of SSF, 0.748 mL of 0.63 mg/mL amylase solution and 4.67 µL of 0.3M CaCl2 solution was shaken at 37 °C for 2 minutes. The sample collection time points were at 0 and 2 minutes. SGF at pH 3 was prepared by adding 862.5 µL of 0.5M KCl solution, 112.5 µL of 0.5M KH_2PO_4 solution, 1.563 mL of 1M $NaHCO_3$ solution,
1.475 mL of 2M NaCl, 50 µL of 0.15M $MgCl_2$ solution, 62.5 µL of 0.5M $(NH_4)_2CO_3$ solution, 162.5 µL of 1M HCl solution, 0.625 µL of 0.3M $CaCl_2$ solution and 45.712 mL of DI water. The gastric master mix consists of 2 mL of SGF, 13.30 mg of pepsin, 0.5 mL of DI water and 1.25 µL of 0.3M $CaCl_2$ solution. The gastric digestion setup follows the salivary digestion where 2.5mL of gastric master mix was added to aliquot and adjusted to pH 3 by addition of 0.1M HCl solution. The gastric digesta was shaken at 37 °C for 2 hours. 0.1M NaOH solution was added after 2 hours of gastric digestion to raise the pH to 8.0, thereby preventing any further pepsin activity. SIF at pH 7 was prepared by adding 850 µL of 0.5M KCl solution,100 µL of 0.5M KH_2PO_4 solution, 5.313 mL of 1M $NaHCO_3$ solution, 1.2 mL of 2M NaCl, 137.5 µL of 0.15M $MgCl_2$ solution, 87.5 µL of 1M HCl solution, 5 µL of 0.3M $CaCl_2$ solution and 42.308 mL of DI water. The intestinal master mix was prepared by mixing 4 mL of SIF, 48.8 mg of bile salts, 25.54 mg pancreatin dissolved in 2 mL of SIF and 10 µL of 0.3M $CaCl_2$ solution. After the completion of salivary and gastric digestion, the intestinal digestion process was initiated by adding 5 mL of SIF to gastric master mix and adjusting its pH to 7.0. The intestinal digesta was shaken at 37 °C for 30 minutes, 1 hour and 2 hours. The intestinal digestions were stopped by adding protease inhibitor solution. All the collected samples were stored in freezer for further characterization.

2.4 Simulated colonic digestion of mucin-terminated microcarriers

Wilkins Chalgren (WC) media was prepared per manufacturer's instructions (Sigma-Aldrich) and deoxygenated in anaerobic chamber for 7 days prior to use. Fed state simulated colonic fluids (FeSSCoF, Biorelevant UK) was prepared per manufacturer directions - 332 mg Tris, 315 mg maleic acid and 59 mg NaOH were dissolved in 27 ml DI water and adjusted to pH to 6.0 by adding 120 µL of 3M HCl. Next, 66 mg of FeSSCoF was added and placed in the anaerobic chamber (Coy Laboratory Products, USA) to dissolve and deoxygenate for at least 48 hours prior to use. Fecal microbiota glycerol stocks from Donor 1 were purchased from Asian Microbiome Library Pte. Ltd. (Singapore). *Slackia equolifaciens DZE* was purchased from DSMZ (Germany) and banked in 35 % glycerol WC media prior to use. To model colonic digestion by the microbiota, 10 ml FeSSCoF was mixed with 10 ml of intestinal digesta, 5 ml of WC broth and 5 ml of OD600 0.1 overnight fecal microbiota (plus *S. equolifaciens* where relevant) from a single donor. The colonic phase fluid was mixed thoroughly by pipetting, split into 4 x 6 ml culture tubes and incubated at 37 °C for 0, 24, 48 and 120 hours.

2.5 Characterization

2.5.1 Ultra-performance liquid chromatography-mass spectrometry (UPLC-MS) quantitation of daidzein

All samples were analysed using a Vanquish™ Duo ultra-high pressure liquid chromatography system coupled to TSQ Quantis™ Triple Quadruple Mass Spectrometer (ThermoFisher Scientific, Waltham, MA). Chromatographic separation was achieved using an ACQUITY UPLC BEH C18, 1.7 µM, 2.1 × 50 mm column (Waters, Milford, MA), maintained at 45 °C. Samples were delivered using injection volumes of 1 µL. Aqueous and organic mobile phases utilized were water containing 0.1 % (v/v) formic acid (mobile phase A) and acetonitrile containing 0.1 % (v/v) formic acid (mobile phase B). Mobile phases were delivered at a flow rate of 0.45 mL/min. The gradient program was as follows: linear gradient from 10 % B to 10 0 % B (0.00 – 2.00 minutes), isocratic at 100 % B (2.00 – 3.00 minutes), and isocratic at 10 % B (3.01 – 4.50 minutes). The MS was operated in ESI positive mode and the source conditions are specified in Table S1. Data for daidzein and their respective internal standards were acquired and analyzed using TraceFinder 4.1 (ThermoFisher Scientific, Waltham, MA). For all UPLC-MS/MS analyses, the peak area of the analyte was expressed as a ratio to the peak area of the internal standard. The multiple reaction monitoring (MRM) transitions and compound-dependent MS parameters of the analytes are also summarized in Table S1.

2.5.2 Sample processing for quantitation of daidzein loaded FCC and microcarriers

Direct DMSO extraction: The daidzein loaded FCC microparticles or daidzein loaded microcarriers were extracted using DMSO solution and centrifuged at 10,000 rpm for 10 minutes to separate supernatant. The supernatant is diluted 1 million times with methanol and internal standard.

Ball milling extraction: The daidzein loaded FCC microparticles or daidzein loaded microcarriers were re-suspended in 20 mL of DMSO solution, and then ball milled for 8 hours to release loaded daidzein, and the supernatant and pellets were separated by centrifugation at 10,000 rpm for 10 minutes. Aliquots, 1 mL supernatant of samples with 1 and 2 washes, were diluted 5000 to 2 million times with methanol and internal standard. Daidzein calibrates were prepared in the relevant digestive matrices to attain final concentrations ranging from 0 – 2 µM. To both samples and calibrates, an equal volume of methanol containing 93.2 -nM of the internal standard (Daidzein-d3) was added, and the final mixture was subjected to UPLC-MS/MS analysis. Each experiment was done in triplicate.

2.5.3 Sample processing for quantitation of daidzein loaded mucin-terminated microcarriers following upper gut digestion via INFOGEST and lower gut colonic fermentation

Aliquots of the digestate collected at the end of the oral, gastric, intestinal and colonic phases were first centrifuged at 3000 rpm for 10 minutes. The supernatant was aspirated and the pelleted microcarriers were subsequently lyophilized for upper gut samples. To release the retained daidzein, 5 mg of the lyophilized microcarriers were extracted with 1 mL DMSO by vortex for 2 minutes. After centrifugation at 3000 rpm for 10 minutes, the supernatant was removed and diluted 500 to 5000 times with methanol. Daidzein and equol calibrants were prepared in the relevant digestive matrices to attain final concentrations ranging from 0 – 2 μM. To both samples and calibrants, an equal volume of methanol containing 93.2 ¬nM of the internal standard (Daidzein-d3) was added, and the final mixture was subjected to UPLC-MS/MS analysis. A two-sample independent t-test conducted on $(BSA\text{-}TA)_4$-mucin and $(BSA\text{-}TA)_8$-mucin where t(df) = 12.0, p > 0.003 and t(df) = 0.9, p > 0.211. In colonic phase, the separated supernatants instead of pellet, at 0, 24, 48 and 120 hours timepoints, were filtered with a sterile 0.22 μm polyethersulfone (PES) filter and subsequently lyophilized for further UPLC-MS/MS analysis.

2.5.4 Raman Spectroscopy

Raman spectra were acquired using a Renishaw inVia confocal Raman microscope. Sample solutions were drop-casted and air dried on a glass slide. A 100x objective lens was used to focus the 532 nm laser excitation beam on the dried sample. The backscattered Raman signal was collected by the CCD-based detector using the same objective lens.

2.5.5 X-Ray Diffraction (XRD)

For XRD analysis, daidzein powder and FCC were used as received, daidzein loaded microcarriers and empty microcarriers were used as dry powder. A Bruker D8 General Area Detector Diffraction System (GADDS) equipped with a Cu-Kα source was used to do XRD analysis of all the powders.

2.5.6 Scanning electron microscopy (SEM)

The surface morphology of all tested microparticles and microcarriers were investigated by FEGSEM, JEOL JSM-7600F in secondary electron imaging mode at the accelerating voltage of 5 to 15 kV. Samples were prepared by depositing a drop of suspension on a silicon wafer and leaving it to dry at a slightly elevated temperature (~35 °C). Before imaging, the samples were coated with an about 5-nm-thick Au film using a sputter coater (JEOL, JFC-1200).

2.5.7 Fluorescence Spectrometry

The measurements of fluorescence intensity were performed using a Duetta Spectrofluorometer (Horiba). The emission spectra were recorded over a range of 595–720 nm wavelengths; excitation wavelength was 590 nm, the emission slit widths was 10 nm, and the scanning speed was 50 nm/min. All measurements were performed using disposable polystyrene cuvettes with optical path length of 10 mm at room temperature (22 °C). All the emission spectra registered had maximal intensity at 620 nm.

2.6 Statistical analysis.

Statistical analysis was performed with Origin software by 2 samples t-test. $p \leq 0.05$ was considered as statistically significant difference.

3. Results and Discussion

3.1 Mucin Subtype Pre-screening for Microcarriers Terminal Layer Development

In this study, the stability of microcarriers coated with different mucin types was investigated under gastrointestinal digestion using simplified INFOGEST. Although several different mucins have been used to address their interfacial behaviour, bovine submaxillary mucin (BSM) and pig gastric mucin (PGM) are the choice of our studies due to their well-characterized compositions and availability from commercial suppliers. Comparing cost, mucin from BSM is more expensive than PGM due to its lower yield and higher purity. Mucin type I from BSM have higher molecular weight followed by Mucin type II and III from PGM. Mucin type II contains 1 % sialic acid unpurified where type III contains between 0.5 and 1.5 % partially purified. Mucin type I forms a clear solution in aqueous environment, whereas mucin type II and III form turbid suspensions.

To quickly screen the efficiency of microcarriers protection from gastrointestinal environment, DQ™ Red BSA was used as cargo because the digestion of this protein may be easily followed by fluorescence spectroscopy.[35] The protection efficiency (PE) was calculated using Equation 1, where I_x is the fluorescence intensity of the samples at the end of digestion and I_0 is the fluorescence intensity of the unprotected DQ-Red BSA at the same digestion time point.

$$\boldsymbol{PE} = \left[\mathbf{1} - \frac{I_x}{I_0}\right] \times \mathbf{100}\% \quad (1)$$

The results are shown in Table 1 (Fluorescence spectra are shown in Figure S1). The PE of $(BSA\text{-}TA)_4$ microcarriers in SGF is 87 % and in SIF the PE is 46 %. Comparing microcarriers coated with three mucin types, those with mucin type I and III show similar PE in SGF of 93 % and 94 %, respectively. In SIF, microcarriers coated with mucin III show better PE of 61 % compared to mucin I of 53 %. However, microcarriers coated with mucin type II, which is not purified, exhibits poorer PE of 79 % in SGF and 13 % in SIF. In a review paper, Svensson *et. al.*[36] provided insights into the impact of mucin type, preparation methods, and surface properties on the adsorption process and the formation of mixed layers, including multilayers, and demonstrated how the presence of impurities can impact the binding affinity of mucin during assembly. Our research findings align with previous studies and demonstrate that the presence of impurities in PGM-based mucin II can directly influence the ability of mucin to form a protective layer and stabilize microcarriers in the gastrointestinal tract.

Table 1. Performance- and cost-efficiency of various microcarriers protecting encapsulated DQ-red BSA from gastrointestinal digestion tested using simplified INFOGEST.

Microcarriers	Protection from simulated gastric fluid (SGF) (%)	Protection from simulated intestinal fluid (SIF) (%)	Mucin Cost[a] (USD/g)
$(BSA\text{-}TA)_4$	87±3	46±2	-
$(BSA\text{-}TA)_4$-Mucin Type I	93±0.2	53±0.9	$1023
$(BSA\text{-}TA)_4$-Mucin Type II	79±4	13±1.4	$2.80
$(BSA\text{-}TA)_4$-Mucin Type III	94±0.4	61±1.4	$7.30

[a] Price of mucin extracted from Merck & Co Inc.

Overall, microcarriers coated with mucin type I and III demonstrate high stability during upper intestinal digestion preventing the release and digestion of DQ-red-BSA cargo. Moving forward, the microcarriers composition of $(BSA\text{-}TA)_4$-mucin III was selected for daidzein encapsulation because it provides the highest intestinal stability and has lower material cost.

3.2 Mucin Subtype Pre-screening for Microcarriers Terminal Layer Development

To understand the nature of interactions between mucin and tannin, Raman spectroscopy was used. The Raman spectra demonstrate that the TA-mucin interaction changes the vibrational frequencies of specific functional groups in both molecules. Figure 1 shows two peaks of TA at 1611 and 1706 cm^{-1}, which may be assigned to the 8*a* mode of C-C stretching in the aromatic ring and the ether C=O stretching[37], respectively, and one peak of mucin at 1664 cm^{-1}, which is primarily attributed to the amide I C=O stretching. Figure 1a shows that the peak at 1611 cm^{-1} shifts to lower wavenumber of 1607 cm^{-1}, while the peaks at 1706 cm^{-1} and 1664 cm^{-1} shift to a higher wavenumber of 1713 cm^{-1} and 1670 cm^{-1}, respectively, with increasing mucin: TA ratio (individual peak-fitting and full Raman spectra are shown in Figure S2). These changes in vibrational frequencies suggest that there are specific interactions between TA and mucin protein backbone.[38] The shift of the aromatic ring peak of TA suggests a hydrophobic interaction between the aromatic ring of TA and hydrophobic patches within mucin. The shift of the C=O peaks of TA and mucin as shown in Figure 1b suggests that the ether group of TA and amide I group of mucin are involved in stronger interactions within the TA-mucin complex.

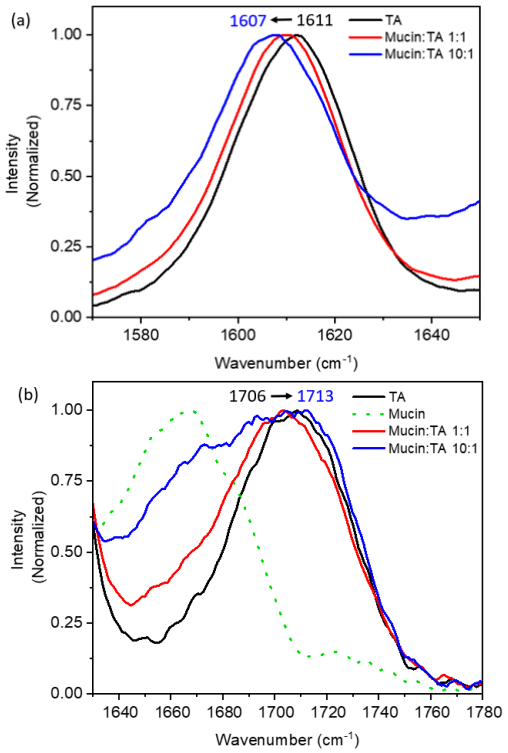

Fig 1. Raman peaks of tannin (TA), mucin and TA-mucin complexes of different ratio showing shifts in a position of (a) TA aromatic ring peak, and (b) ether C=O peak of TA and amide I peak of mucin. (Arrows indicate direction of shift in peak positions)

3.3 Evaluation of daidzein loading in porous calcium carbonate template

We evaluated the loading capacity (LC) of porous FCC microparticles for daidzein upon its absorption from a solution in DMSO followed by drying. LC was measured upon crushing the particles in a ball mill filled with DMSO and determining the daidzein amount extracted into DMSO by UPLC-MS. LC of porous FCC microparticles is defined here as wt.% of daidzein in the powders as shown in Equation 2:

$$LC = \frac{Weight\ of\ absorbed\ daidzein}{Weight\ of\ (CaCO_3 + absorbed\ daidzein)} \times 100\% \quad (2)$$

Our findings reveal a LC of 21.6 ± 1.8 % for daidzein in FCC microparticles. To further investigate the efficiency of daidzein retention, we challenge the daidzein-loaded FCC microparticles with consecutive DMSO washings. Retention efficiency (RE) of porous FCC microparticles is defined as the percentage of daidzein amount retained in the washed powder to the amount of daidzein initially absorbed by the powder as shown in Equation 3:

$$RE = \frac{Retained\ daidzein\ weight}{Absorbed\ daidzein\ weight} \times 100\% \quad (3)$$

Our results show a RE of 36 % and 7 % after one and two washes, respectively. It is important to note that our study successfully demonstrates loading of small hydrophobic molecules into FCC microparticles. In our previous investigation we demonstrated

that FCC (same as SRCC3) exhibits LC of 11 % for water-soluble protein, lactoferrin, with RE of 74 % after 2 cycles of washing with DI water.[30] Therefore, FCC demonstrate substantially higher LC for hydrophobic small molecules than macromolecules but subsequent higher washout from the matrix.

3.4 Preparation of microcarriers coated with mucin

Daidzein-loaded FCC microparticles were used as a template to prepare protein-polyphenol microcarriers coated with mucin. Attempt to perform LbL assembly over FCC microparticles loaded with 21.6 wt. % of daidzein failed. Possible reasons could be interference of hydrophobic daidzein particles adsorbed on the FCC surface with the coating solution preventing wetting, or the necessity for FCC to have a cleaner surface with open porosity to promote strong adsorption of multilayer-forming molecules. Therefore, it is critical to remove excess of the hydrophobic particles through washing with DMSO to ensure proper wetting of the surface though it reduces the amount of loaded daidzein to 7.8 wt. % (LC of 21.6 % and RE of 36 % after one DMSO wash, 21.6 x 0.36 ≈ 7.8). Going forward, a single DMSO washing step was performed prior to the LbL assembly.

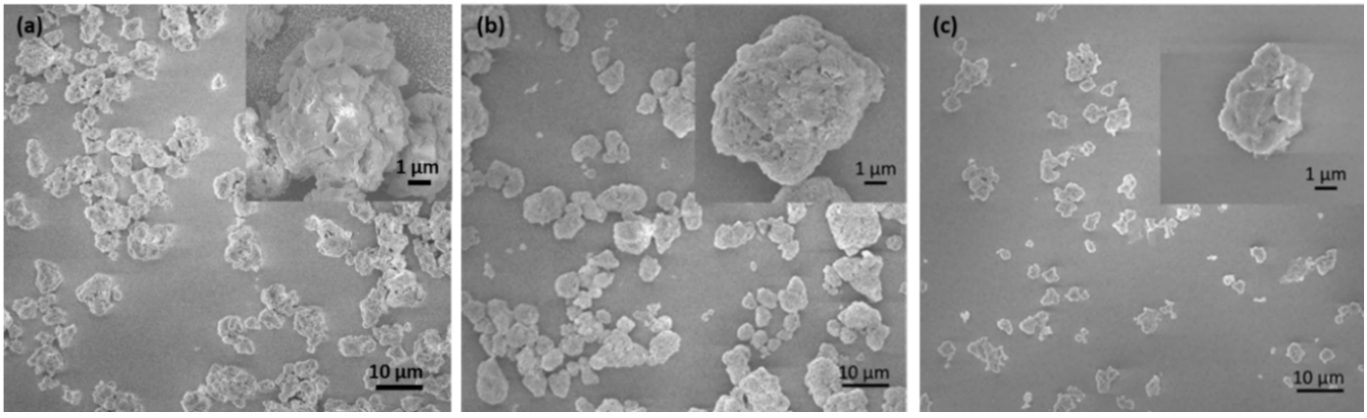

Fig 2: Scanning electron microscopy images of (a) functionalized calcium carbonate (FCC) porous templates, the daidzein loaded microcarriers coated with (bovine serum albumin-tannin)$_4$-mucin shells (b) before and (c) after FCC removal with 1M HCl.

Firstly, four BSA-TA bi-layers were assembled, followed by coating with mucin. Figure 2 shows the SEM images of initial FCC particles and daidzein-loaded microcarriers. Porous FCC particles used in this work as templates are irregularly shaped having size of approximately 6 to 10 µm, as shown previously.[30] For the ease of comparison, their SEM image is shown here in the Figure 2-a. Daidzein-loaded particles with assembled (BSA-TA)$_4$-mucn shell resemble the initial porous FCC templates. Subsequently, the suspension was treated with hydrochloric acid to remove the FCC cores. As evident from SEM images, the size of the resulted microcarriers shrank by ~50 % to approximately 3 to 5 µm but the overall structure and fidelity of the microcarriers remain intact. Therefore, the LbL assembly of BSA-TA-mucin shells forms stable structures that are unaffected by the removal of the FCC cores. It is worth noting that (BSA-TA)$_4$-mucin notation used here and below describes the sequence of molecules introduction. Previously, we have shown that BSA-TA film thickness increases linearly with each introduction.[28] However, the resulted shells may not necessarily have a distinct layered structure.

3.5 Evaluation of daidzein in mucin coated protein-tannin microcarriers

To check whether the microcarriers contain daidzein, we performed XRD analysis. The XRD of the daidzein powder in Figure 3 (black line) shows sharp peaks at various angles, confirming the highly crystalline nature of the compound.[39] The crystallite sizes of daidzein powder calculated using Debye–Scherrer equation at 2θ 15.8 °, 24.5 °, and 29.8 ° were 69 nm, 52 nm, and 51 nm, respectively. In contrast, the powder containing empty (BSA-TA)$_4$-mucin microcarriers in Figure 3 (red line) showed a broad peak, indicating its amorphous nature. The powder containing daidzein-loaded microcarriers in Figure 3 (blue line) showed a superposition of the broad peak resembling that of the empty microcarriers with sharp peaks at the same characteristic positions as in daidzein powder. We take it as evidence of successful daidzein retention. Interestingly, the daidzein crystallite sizes calculated at the same 2θ of 15.8 °, 24.5 °, and 29.8 ° were 30.7 nm, 33.4 nm, and 32.6 nm, respectively. This reduction in crystallite size compared to initial daidzein powder could be attributed to the confined spaces within the pores of FCC template which may have restricted the growth of the daidzein crystallites happening upon DMSO evaporation. It is worth to note that there were no peaks observed characteristic for the porous FCC template shown in Figure 3 (pink line), indicating that its content within microcarriers after the HCl treatment process is below the detection limit of XRD.

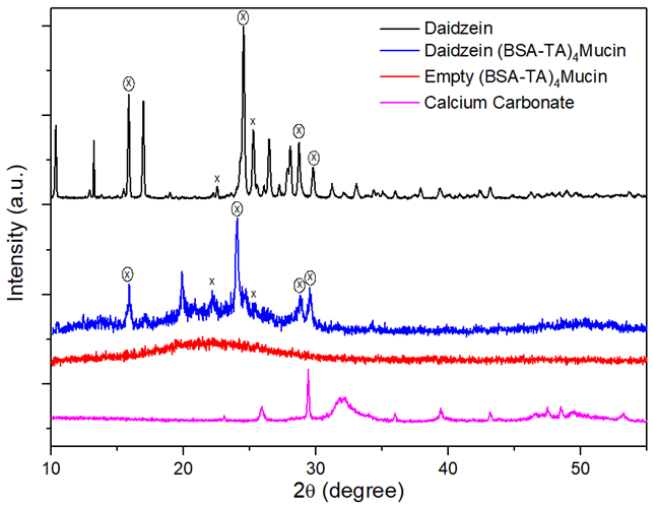

Fig 3: Powder X-ray diffraction patterns of daidzein powder (black), daidzein loaded (bovine serum albumin-tannin)$_4$-mucin microcarriers (blue), empty (bovine serum albumin-tannin)$_4$-mucin microcarriers (red) and functionalized calcium carbonate (pink).

The amount of daidzein in the microcarriers was evaluated by measuring the daidzein amount extracted into DMSO using UPLC-MS. Here we employed two different extraction methods: direct DMSO extraction from a suspension of microcarriers and their ball-milling in DMSO. Direct extraction yielded 12.4 mg of daidzein per 60 mg of microcarriers, while ball-milling yielded 32.3 mg of daidzein. These findings suggest that the ball-milling method breaks microcarriers mechanically (Figure S3) and therefore allows a more effective extraction. It is worth noting that the amount of extracted daidzein may vary depending on the extraction method used, and the ball-milling method may be more suitable for certain types of samples.

We would like to highlight here that the daidzein content in FCC after one DMSO wash was ~ 7.8 wt.%. However, daidzein content in the final microcarriers is ~54 wt. % (32.3 mg of daidzein out of 60 mg of microcarriers). This is due to the fact that FCC template was decomposed upon HCl treatment, and the weight of remaining multilayer shell is just ~10 wt.% of the initial FCC template, as shown previously.[30]

3.6 *In vitro* digestion of mucin coated protein-polyphenol microcarriers with daidzein

We have evaluated daidzein retention in microcarriers upon simulated gastrointestinal digestion separating the remaining microcarriers by centrifugation and measuring the daidzein amount extracted into DMSO upon their ball-milling using UPLC-MS. Figure 4 shows the RE of daidzein after 2 minutes in simulated salivary fluid (SSF) followed by 2 hours of gastric and 2 hours of intestinal digestion for three different compositions of microcarriers, (BSA-TA)$_8$, (BSA-TA)$_8$-mucin, and (BSA-TA)$_4$-mucin. The RE of daidzein in (BSA-TA)$_8$ was found to be 87 ± 8.7 %, 63 ± 6.3 % and 46 ± 4.6 %, respectively. In contrast, the RE of daidzein in (BSA-TA)$_8$-mucin was 94 ± 6.5 %, 78 ± 8.1 % and 71 ± 8.2 %, respectively. When the number of protein-polyphenol bilayers is reduced to 4, the RE remains high at 86 ± 10.9 %, 76 ± 3.4 % and 68 ± 2.3 %, respectively. There is no statistical difference in the amount of daidzein retained in (BSA-TA)$_4$-mucin and (BSA-TA)$_8$-mucin at the end of both gastric and intestinal phase. Thus, 4 bilayers may be sufficient to provide adequate retention for encapsulated bioactive. This has implications for reducing the material cost and simplifying the manufacturing process of mucin-terminated microcarriers.

Overall, the mucin-coated microcarriers exhibited remarkable resistance against simulated salivary, gastric, and intestinal digestion. This suggests that coating microcarriers with mucin may be a promising strategy to prevent daidzein transition into mixed micellar phase and its subsequent absorption in the small intestine enhancing the bioaccessibility in the colon. It is worth noting that without any protection, only 17 % of daidzein is extracted at the end of digestion.

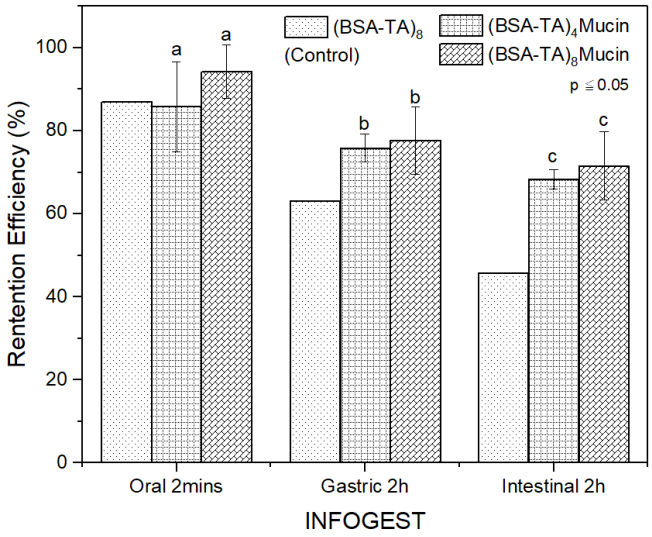

Fig 4: Efficiency of microcarriers made of (bovine serum albumin-tannin)$_n$-mucin in daidzein retention across INFOGEST digestion phases measured by UPLC-MS. Means indicated by different superscript letters are significantly different ($p \leq 0.05$).

3.7 *In vitro* colonic release of mucin coated protein-polyphenol microcarriers with daidzein and conversion into equol

To evaluate the release of daidzein in the colon, mucin coated protein-polyphenol microcarriers that had been subjected to upper gut INFOGEST digestion were incubated with simulated colonic fluid (Biorelevant, FeSSCoF), fecal microbiota from a healthy non-equol-producing donor and we introduced *Slackia equolifaciens*, a bacteria encoding all three reductases needed to convert daidzein into equol, into all the colonic setups. During initial pilots to first confirm *S. equolifaciens*' ability to convert daidzein into equol, *S. equolifaciens* alone was interestingly unable to convert unprotected daidzein into equol but could do so when present in donor fecal microbiota. After 120 hours, the unprotected daidzein was converted into equol as shown in Table S2 suggests that *S. equolifaciens* activates expression of the reductase enzymes while interacting with

other gut microbiota members, and that interactions between *S. equolifaciens* and donors' microbes promoted efficient daidzein to equol conversion. Next, we evaluate whether *S. equolifaciens* in donor microbiota could similarly convert any daidzein released from microcarriers into equol. Figure 5 shows our in-vitro colonic phase data suggests that trace amounts of daidzein (≤0.01 mg)) released from our microcarriers (red line) is converted into equol under *in vitro* colonic conditions mimicking that of equol producers. The low detection of daidzein in supernatant of colonic phase might also be due to a low solubility limit of daidzein in colonic fluid. The saturated solubility of daidzein is approximately 0.009 mg[40] in the colonic phase, which is similar to the range of daidzein measured in colonic phase time points. Hence, this may explain our observation of limited daidzein release in the colonic phase. Figure 5 also shows 56.4 % conversion into equol only after 48 hours (black bars). The amount of equol produced increased up until 120 hours (last time point measured) but was a fraction of the maximum amount of equol producible from the daidzein released. However, the production took up to 48 hours *in vitro*, which is on the tail end of normal *in vivo* physiological human gut transit times.

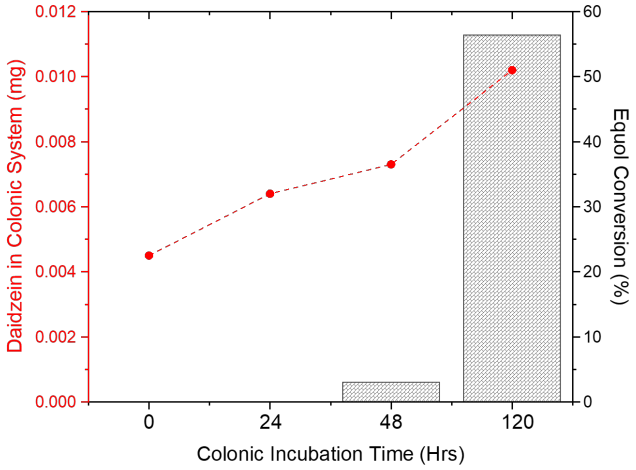

Figure 5: Daidzein measured and S-equol conversion in the colonic set-ups at different incubation timepoints with donor fecal microbiota and *Slackia equolifaciens*.

Conclusions

We present the study on development of BSA-TA multilayer microcarriers coated with mucin as an effective oral delivery system for the small hydrophobic molecule, daidzein. In the developmental stage of microcarrier material, mucin type III was found to be a cost-effective candidate with the highest protection efficiency against gastrointestinal digestion. The formation of a TA-mucin complex was confirmed by Raman spectroscopy. The LC of daidzein in the porous FCC template was found to be 21.6 ± 1.8 %, and the RE was 36 % after one wash with DMSO, and 7 % after two washes. The SEM analysis of LbL-assembled microcarriers established their size in the range from 3 to 5 µm. XRD analysis confirmed entrapment of nanocrystalline daidzein in the microcarriers, while UP-LCMS quantified the daidzein content as 54 wt.%. The mucin-coated microcarriers showed high stability in simulated salivary, gastric, and small intestinal phases. Without the mucin coating layer, the control $(BSA\text{-}TA)_8$ had a RE of 46 ± 4.6 % at the end of intestinal phase. The RE of daidzein in $(BSA\text{-}TA)_8$-mucin and $(BSA\text{-}TA)_4$-mucin was 71 ± 8.2 % and 68 ± 2.3 %, respectively. These results highlight the importance of mucin coating layer in elevating stability upon gastrointestinal digestion compared to the control. In colonic studies, we confirm the release of daidzein from the microcarriers by a distinct fecal microbiota. The donor communities are non-equol producers, and the addition of *S. equolifaciens* into donor microbiota demonstrated daidzein conversion to equol at ≥48 hours. However, further work needs to be conducted to optimize colonic release and modelling conditions as well as evaluation of the release kinetics of daidzein in the presence of isolated mucinase enzyme, will provide insights on the mechanism of colon-specific release. We believe that the developed material can be extended to encapsulation and colon-targeted delivery of a variety of small hydrophobic molecules, e.g. therapeutics or nutraceuticals, enabling modulation of gut microbiome communities and metabolism to alter host health outcomes.

Author Contributions

Conceptualization – S.H. Lim, G.J.M. Yong, M. V. Kiryukhin.; Funding acquisition - S.H. Lim, G.J.M. Yong.; Investigation - S.H. Lim, G.J.M. Yong, C. Y. Chia, G. S. Subramanian, S.M. Man, G. Oh, E.J.Y. Cheong; methodology - S.H. Lim, G.J.M. Yong, M. V. Kiryukhin.; Data curation - S.H. Lim, G.J.M. Yong, M. V. Kiryukhin; Project administration - S.H. Lim, G.J.M. Yong.; Supervision - S.H. Lim, G.J.M. Yong., M. V. Kiryukhin.; Validation - S.H. Lim, G.J.M. Yong. C. Y. Chia, G. S. Subramanian, S.M. Man, G. Oh, E.J.Y. Cheong; Visualization - S.H. Lim, G.J.M. Yong.; Validation - S.H. Lim, G.J.M. Yong. C. Y. Chia, G. S. Subramanian, G. Oh; Writing of original draft - S.H. Lim.; Writing review & editing – All the authors contributed equally.

Conflicts of interest

The authors declare that there are no conflicts of interests.

Acknowledgements

The authors acknowledge Ms. Chew Li Tian and Dr Fengxia Wei from Institute of Material Science and Engineering for their support in XRD characterization. The authors would like to thank Singapore Institute of Food and Biotechnology Innovation, SIFBI, for Seed Grant financial support of this work (Project: SC34/21-107400).

References

1. J. Liggins, L. Bluck, S. Runswick, C. Atkinson, W. Coward and S. Bingham, *British Journal of Nutrition*, 2000, **84**, 717-725.

2. J. Liggins, L. J. Bluck, S. Runswick, C. Atkinson, W. A. Coward and S. A. Bingham, *The Journal of nutritional biochemistry*, 2000, **11**, 326-331.
3. E. J. Choi and G. H. Kim, *Mol Med Rep*, 2014, **9**, 328-332.
4. Y. Ungar, O. F. Osundahunsi and E. Shimoni, *Journal of Agricultural and Food Chemistry*, 2003, **51**, 4394-4399.
5. Y. Tan, X. Zhang and W. S. Cheang, *Chinese Medicine*, 2022, **17**, 95.
6. M. Hämäläinen, R. Nieminen, P. Vuorela, M. Heinonen and E. Moilanen, *Mediators of inflammation*, 2007, **2007**.
7. R. Sanatkar, G. Rahimi Kalateh Shah Mohammad, E. Karimi, E. Oskoueian and R. Hendra, *Polymer Bulletin*, 2021, 1-15.
8. C. Bao, H. Namgung, J. Lee, H.-C. Park, J. Ko, H. Moon, H. W. Ko and H. J. Lee, *Journal of Agricultural and Food Chemistry*, 2014, **62**, 3759-3767.
9. F. Qiu, X.-y. Chen, B. Song, D.-f. Zhong and C.-x. Liu, *Acta Pharmacologica Sinica*, 2005, **26**, 1145-1152.
10. P. Janning, U. Schuhmacher, A. Upmeier, P. Diel, H. Michna, G. Degen and H. Bolt, *Archives of toxicology*, 2000, **74**.
11. X. Li, Q. Shen, D. Yuan, A. Ma and W. Jia, *Chromatographia*, 2008, **68**, 201-205.
12. D. W. Ningtyas, S. Hati and S. Prakash, *Food Chemistry*, 2021, **343**, 128553.
13. K. R. Walsh, Y. C. Zhang, Y. Vodovotz, S. J. Schwartz and M. L. Failla, *Journal of agricultural and food chemistry*, 2003, **51**, 4603-4609.
14. E. Fernández-García, I. Carvajal-Lérida and A. Pérez-Gálvez, *Nutrition research*, 2009, **29**, 751-760.
15. H. Cheng, S. Huang and G. Huang, *Journal of Enzyme Inhibition and Medicinal Chemistry*, 2019, **34**, 1590-1596.
16. Z. Zhang, Y. Huang, F. Gao, H. Bu, W. Gu and Y. Li, *Nanoscale*, 2011, **3**, 1780-1787.
17. Y. Ma, X. Zhao, J. Li and Q. Shen, *International Journal of Nanomedicine*, 2012, 559-570.
18. Q. Wang, W. Liu, J. Wang, H. Liu and Y. Chen, *Nanoscale Research Letters*, 2019, **14**, 1-10.
19. G. P. Panizzon, F. Giacomini Bueno, T. Ueda-Nakamura, C. V. Nakamura and B. P. Dias Filho, *Pharmaceutics*, 2019, **11**, 492.
20. K. D. Setchell and C. Clerici, *The Journal of nutrition*, 2010, **140**, 1355S-1362S.
21. B. Mayo, L. Vázquez and A. B. Flórez, *Nutrients*, 2019, **11**, 2231.
22. G. Rimbach, C. Boesch-Saadatmandi, J. Frank, D. Fuchs, U. Wenzel, H. Daniel, W. L. Hall and P. D. Weinberg, *Food and Chemical Toxicology*, 2008, **46**, 1308-1319.
23. J.-R. Zhou, L. Li and W. Pan, *The American journal of clinical nutrition*, 2007, **86**, 882S-888S.
24. K. D. Setchell and A. Cassidy, *The journal of nutrition*, 1999, **129**, 758S-767S.
25. M. Wahlgren, M. Axenstrand, Å. Håkansson, A. Marefati and B. Lomstein Pedersen, *Pharmaceutics*, 2019, **11**, 95.
26. P. Labuschagne, *Food Research International*, 2018, **107**, 227-247.
27. E. Kilic, M. V. Novoselova, S. H. Lim, N. A. Pyataev, S. I. Pinyaev, O. A. Kulikov, O. A. Sindeeva, O. A. Mayorova, R. Murney, M. N. Antipina, B. Haigh, G. B. Sukhorukov and M. V. Kiryukhin, *Scientific Reports*, 2017, **7**, 44159.
28. H. H. Lau, R. Murney, N. L. Yakovlev, M. V. Novoselova, S. H. Lim, N. Roy, H. Singh, G. B. Sukhorukov, B. Haigh and M. V. Kiryukhin, *Journal of Colloid and Interface Science*, 2017, **505**, 332-340.
29. M. V. Lomova, A. I. Brichkina, M. V. Kiryukhin, E. N. Vasina, A. M. Pavlov, D. A. Gorin, G. B. Sukhorukov and M. N. Antipina, *ACS Applied Materials & Interfaces*, 2015, **7**, 11732-11740.
30. M. V. Kiryukhin, S. H. Lim, H. H. Lau, M. Antipina, Y. W. Khin, C. Y. Chia, P. Harris, M. Weeks, C. Berry and D. Hurford, *Journal of Colloid and Interface Science*, 2021, **594**, 362-371.
31. M. Farzan, R. Roth, G. Québatte, J. Schoelkopf, J. Huwyler and M. Puchkov, *Pharmaceutics*, 2019, **11**, 32.
32. M. Lundin Johnson, D. Noreland, P. Gane, J. Schoelkopf, C. Ridgway and A. Millqvist Fureby, *Food & Function*, 2017, **8**, 1627-1640.
33. C. Butnarasu, P. Petrini, F. Bracotti, L. Visai, G. Guagliano, A. Fiorio Pla, E. Sansone, S. Petrillo and S. Visentin, *Advanced Healthcare Materials*, 2022, **11**, 2200340.
34. A. Brodkorb, L. Egger, M. Alminger, P. Alvito, R. Assunção, S. Ballance, T. Bohn, C. Bourlieu-Lacanal, R. Boutrou and F. Carrière, *Nature protocols*, 2019, **14**, 991-1014.
35. M. Minekus, M. Alminger, P. Alvito, S. Ballance, T. Bohn, C. Bourlieu, F. Carrière, R. Boutrou, M. Corredig and D. Dupont, *Food & function*, 2014, **5**, 1113-1124.
36. O. Svensson and T. Arnebrant, *Current Opinion in Colloid & Interface Science*, 2010, **15**, 395-405.
37. A. Espina, S. Sanchez-Cortes and Z. Jurašeková, *Molecules*, 2022, **27**, 279.
38. J. Yeom, A. Choe, S. Lim, Y. Lee, S. Na and H. Ko, *Science Advances*, 2020, **6**, eaba5785.
39. Y. Bhalla, K. Chadha, R. Chadha and M. Karan, *Heliyon*, 2019, **5**, e02669.
40. G.-D. Yang, Y.-R. Huang, G.-J. Nan, H.-J. Chen, A.-G. Zeng and X.-L. Bian, *Journal of Molecular Liquids*, 2013, **180**, 160-163.